RAB3A Regulates Melanin Exocytosis and Transfer Induced by Keratinocyte-Conditioned Medium

Luís C. Cabaço[1], Liliana Bento-Lopes[1], Matilde V. Neto[1], Andreia Ferreira[1], Wanja B.L. Staubli[1], José S. Ramalho[1], Miguel C. Seabra[1] and Duarte C. Barral[1]

Skin pigmentation is imparted by melanin and is crucial for photoprotection against UVR. Melanin is synthesized and packaged into melanosomes within melanocytes and is then transferred to keratinocytes (KCs). Although the molecular players involved in melanogenesis have been extensively studied, those underlying melanin transfer remain unclear. Previously, our group proposed that coupled exocytosis/phagocytosis is the predominant mechanism of melanin transfer in human skin and showed an essential role for RAB11B and the exocyst tethering complex in this process. In this study, we show that soluble factors present in KC-conditioned medium stimulate melanin exocytosis from melanocytes and transfer to KCs. Moreover, we found that these factors are released by differentiated KCs but not by basal layer KCs. Furthermore, we found that RAB3A regulates melanin exocytosis and transfer stimulated by KC-conditioned medium. Indeed, KC-conditioned medium enhances the recruitment of RAB3A to melanosomes in melanocyte dendrites. Therefore, our results suggest the existence of two distinct routes of melanin exocytosis: a basal route controlled by RAB11B and a RAB3A-dependent route, stimulated by KC-conditioned medium. Thus, this study provides evidence that soluble factors released by differentiated KCs control skin pigmentation by promoting the accumulation of RAB3A-positive melanosomes in melanocyte dendrites and their release and subsequent transfer to KCs.

JID Innovations (2022);**2:**100139 doi:10.1016/j.xjidi.2022.100139

INTRODUCTION

The skin pigmentary system ensures protection against UVR-induced damage and hence, the onset of skin cancer (Del Bino et al., 2018; Narayanan et al., 2010). The photoprotective pigment melanin is synthesized within melanocytes and packaged inside specialized membrane-bound lysosome-related organelles, termed melanosomes (Hearing, 2005; Marks and Seabra, 2001; Raposo and Marks, 2002). Melanocytes reside in the basal layer of the epidermis, sparsely distributed at an approximately 1:40 ratio among keratinocytes (KCs), forming epidermal–melanin units (Del Bino et al., 2018; Fitzpatrick and Breathnach, 1963). Fully melanized melanosomes are transported from the perinuclear region of melanocytes to the dendrites and then transferred to KCs, where melanin granules form a supranuclear cap that absorbs and scatters UVR, protecting nuclear DNA from damage (Park et al., 2009; Scott, 2003). Thus, melanin biogenesis and transfer must be tightly regulated to sustain skin pigmentation and ensure efficient photoprotection. To facilitate this, basal KCs contact and wrap melanocyte dendrites and dendritic spine-like structures, inducing transient calcium signals in these melanocyte structures, thus regulating melanin transfer (Belote and Simon, 2020; Joshi et al., 2007). Moreover, multivesicular bodies in KCs were found to polarize to contact sites with melanocytes, and KC-derived small extracellular vesicles were observed surrounding stubby melanocyte spine-like structures, thereby inducing melanogenesis (Belote and Simon, 2020; Lo Cicero et al., 2015). In contrast to local KC–melanocyte signaling, exposure to UVR enhances the secretion of soluble factors by KCs. These include endothelin-1 and α-melanocyte–stimulating hormone, which act to increase melanin synthesis in a process known as adaptive pigmentation or tanning (Hirobe, 2014; Taisuke and Hearing, 2011; Yamaguchi and Hearing, 2009). In this process, α-melanocyte–stimulating hormone binds to melanocortin-1 receptor on the surface of melanocytes, stimulating melanogenesis and subsequently increasing melanin transfer to KCs (Mosca et al., 2020). Despite this feedback between melanogenesis and melanin transfer, none of the identified KC-derived factors has been shown to exclusively stimulate melanin transfer from melanocytes to KCs without influencing melanin synthesis.

Although the mechanism of melanin transfer continues to be debated, we proposed that the predominant mode in human skin is coupled exocytosis/phagocytosis (Moreiras et al., 2022, 2021; Tarafder et al., 2014). Before melanin is

[1]*iNOVA4Health, NOVA Medical School, Faculdade de Ciências Médicas, NMS, FCM, Universidade NOVA de Lisboa, Lisboa, Portugal*

Correspondence: Duarte C. Barral, NMS Research Center, NOVA Medical School, Faculdade de Ciências Médicas, Universidade NOVA de Lisboa, Campo dos Mártires da Pátria 130, Lisboa 1169-056, Portugal. E-mail: duarte.barral@nms.unl.pt

Abbreviations: CO_2, carbon dioxide; FBS, fetal bovine serum; FCM, fibroblast-conditioned medium; HEKn, human neonatal epidermal keratinocyte; HEMn-DP, human neonatal epidermal darkly pigmented melanocyte; KC, keratinocyte; KCM, keratinocyte-conditioned medium; miRNA, microRNA; MKCM, melanocyte-/keratinocyte-conditioned medium; pKCM, primary keratinocyte-conditioned medium; siRNA, small interfering RNA

Received 25 May 2021; revised 26 April 2022; accepted 27 April 2022; accepted manuscript published online XXX; corrected proof published online XXX

Cite this article as: JID Innovations 2022;2:100139

transferred, melanosomes are transported to melanocyte dendrites, where they are tethered to the cortical actin cytoskeleton through the tripartite complex RAB27A/melanophilin/myosin Va (Barral and Seabra, 2004; Hume et al., 2007). However, at least in two-dimensional melanocyte/KC cocultures, RAB27A is not essential for melanin exocytosis and subsequent transfer to KCs (Tarafder et al., 2014). In search of potential regulators, we found that RAB11B and the exocyst tethering complex control melanin exocytosis and transfer (Moreiras et al., 2019; Tarafder et al., 2014).

The secretory Rab protein RAB3A was shown by electron microscopy to localize to mature melanosome membranes, although the functional implications of this localization have not been elucidated (Araki et al., 2000; Fukuda, 2008). RAB3A is present in melanosome-containing fractions with several SNAREs, including VAMP-2, SNAP-25, SNAP-23, Syntaxin-4, and α-SNAP (Scott and Zhao, 2001). The cofractionation of SNAREs and RAB3A from mature melanosomes strongly suggests a role for this protein in melanin exocytosis. RAB3A was also described to regulate the *trans*-SNARE complex assembly, which promotes vesicle fusion with the plasma membrane (Hong, 2005). Intriguingly, RAB3 regulates the exocytosis of neurotransmitters in neurons, hormone release in endocrine cells, and insulin secretion in pancreatic β cells (Fukuda, 2008). Moreover, a RAB3A-dependent complex is required for conventional lysosome exocytosis during plasma membrane repair (Encarnação et al., 2016; Escrevente et al., 2021). Interestingly, after RAB27A-mediated transport, RAB3A was shown to be essential for the exocytosis of another type of lysosome-related organelle, namely dense cores, in sperm cells (Quevedo et al., 2019). Furthermore, in endothelial cells, Weibel–Palade bodies, which are also lysosome-related organelles, were shown to require cooperation between RAB27A, RAB3A, and RAB3D to be secreted (Delevoye et al., 2019; Raposo et al., 2007; Zografou et al., 2012).

In this study, we found that soluble factors present in KC-conditioned medium (KCM) induce melanin exocytosis and transfer from melanocytes to KCs in a RAB3A-dependent and RAB11B-independent manner. Our results also suggest that differentiated KCs release these soluble factors to induce melanin transfer from melanocytes, thereby enhancing skin pigmentation. Thus, we provide evidence to support a KCM-stimulated melanin exocytosis pathway controlled by RAB3A, distinct from RAB11B-dependent non-KCM–stimulated basal melanin exocytosis.

RESULTS

KCM enhances melanin exocytosis from melanocytes

Previously, KC-derived soluble factors were shown to increase melanogenesis in melanocytes (Hirobe, 2014; Taisuke and Hearing, 2011; Yamaguchi and Hearing, 2009), and therefore, we began by evaluating their effect on stimulating melanin exocytosis. To do so, we obtained KCM by culturing XB2 mouse KCs for 3 days. We then cultured melan-ink4a mouse melanocytes in KCM and assessed melanin secretion. Both RPMI and DMEM media were used as controls because the former is the basis of melanocyte growth medium and the latter is used to culture XB2 KCs. To rule out the possibility that the differences observed in exocytosed melanin levels are a consequence of increased melanogenesis, we also quantified intracellular melanin levels.

We first observed that melanocytes cultured in DMEM show a significant 3.5-fold increase in exocytosed melanin (Figure 1a) and twice the amount of intracellular melanin (Figure 1b) compared with melanocytes cultured in RPMI. Notably, comparing RPMI and DMEM media composition, DMEM contains 3.5 times more L-tyrosine, which is the initial substrate of the key melanogenic enzyme tyrosinase (Hirobe, 2014; Taisuke and Hearing, 2011; Yamaguchi and Hearing, 2009). These enhanced intracellular melanin levels of melanocytes cultured in DMEM were also reported by others (Skoniecka et al., 2021). Interestingly, when melanocytes are cultured in KCM, the levels of exocytosed melanin are 2.5 times higher (Figure 1a and c), whereas the amount of intracellular melanin is 50% lower than that of melanocytes cultured in DMEM (Figure 1b and d). This result suggests that KCM stimulates melanin exocytosis and that this effect cannot be justified by an increase in melanin synthesis.

Next, to test the specificity of melanin exocytosis stimulation by KCM, we cultured melan-ink4a mouse melanocytes with other DMEM-based–conditioned media, namely mouse embryonic fibroblast-conditioned medium (FCM) and conditioned medium from melan-ink4a melanocyte/XB2 KC cocultures (i.e., melanocyte-/KC-conditioned medium [MKCM]). Similar to KCs, dermal fibroblasts are known to release soluble factors that regulate melanogenesis (Taisuke and Hearing, 2011; Yamaguchi and Hearing, 2009). MKCM was used to test whether the crosstalk between melanocytes and KCs affects melanin exocytosis. Interestingly, we observed that KCM induces double the amount of melanin exocytosis relative to FCM and MKCM (Figure 1c). Moreover, melanocytes cultured in MKCM or KCM have similar intracellular melanin levels, and melanocytes cultured with FCM have twice the amount of intracellular melanin as that cultured in MKCM or KCM (Figure 1d). Taken together, these results confirm that KCM contains factors that stimulate melanin exocytosis from melanocytes. We next evaluated whether these factors are soluble factors or factors carried by extracellular vesicles. Indeed, KC-derived extracellular vesicles carrying microRNAs (miRNAs) were shown to stimulate melanogenesis in melanocytes and significantly increase the expression of RAB27A, which is required for melanosome tethering to cortical actin before transfer to KCs (Lo Cicero et al., 2015). To address this question, we ultracentrifuged KCM and MKCM, collected the supernatant (S100 fraction), and resuspended the pellet containing extracellular vesicles (P100 fraction) in DMEM. Melan-ink4a mouse melanocytes were subsequently cultured in MKCM or KCM complete media or with S100 or P100 fractions. We found that S100 fractions from KCM and MKCM stimulate amounts of melanin exocytosis similar to those of the respective complete media (Figure 1e). In contrast, we observed only a slight increase in melanin exocytosis from melanocytes incubated with P100 fractions of KCM or MKCM compared with those incubated in DMEM, albeit not statistically significant (Figure 1e). Importantly, KCM S100 fraction induces double the amount of melanin exocytosis from melanocytes, when compared with MKCM S100 fraction, further indicating that KCM has a higher amount of or even different soluble factors

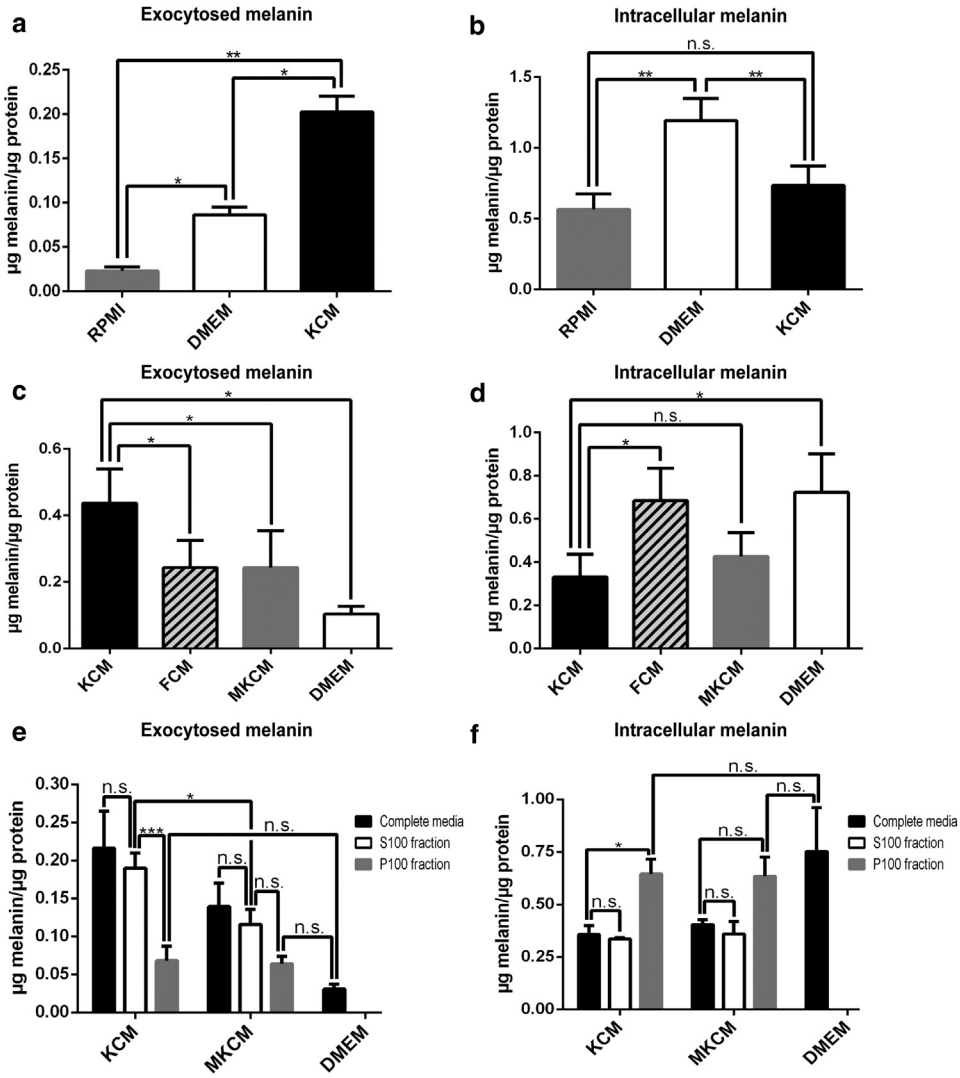

Figure 1. KCM stimulates melanin exocytosis from melanocytes. (**a**) Exocytosed and (**b**) intracellular melanin levels of melan-ink4a melanocytes cultured in different nonconditioned media (RPMI or DMEM) or KCM. (**c**) Exocytosed and (**d**) intracellular melanin levels of melan-ink4a melanocytes cultured in DMEM or different DMEM-based conditioned media (KCM, FCM, or MKCM). (**e**) Exocytosed and (**f**) intracellular melanin levels of melan-ink4a melanocytes cultured in DMEM (control), KCM, or MKCM complete media or with soluble fractions (S100) or pellet fractions (P100) collected after ultracentrifugation. After 3 days of incubation with the indicated culture media, melanocyte melanin levels were quantified by fluorescence spectroscopy as described in the Materials and Methods. Melanin amounts (in µg) were normalized by total protein (also in µg). The plots display the mean ± SD of at least three independent experiments. Data were analyzed with one-way ANOVA for **a, b, c,** and **d** or two-way ANOVA for **e** and **f.** $*P < 0.05$, $**P < 0.01$, and $***P < 0.0001$. FCM, fibroblast-conditioned medium; KCM, keratinocyte-conditioned medium; MKCM, melanocyte-/keratinocyte-conditioned medium; n.s., nonsignificant.

from those of MKCM (Figure 1e). Overall, these results suggest that the effect on melanin exocytosis induced by KCM is mediated mainly, if not only, by soluble factors. Conversely, extracellular vesicles present in KCM can only induce a slight but nonsignificant increase in melanin exocytosis, in addition to a marked increase in melanogenesis (Figure 1f), already reported by others (Lo Cicero et al., 2015).

KCM stimulates melanin exocytosis in a RAB3A-dependent manner

We next aimed to further dissect the molecular machinery involved in melanin exocytosis from melanocytes, in particular on KCM stimulation. Previously, we implicated RAB11B in melanin exocytosis from melanocytes cultured in RPMI (Moreiras et al., 2019; Tarafder et al., 2014). In addition, it has been suggested that RAB3A plays a role in melanin exocytosis (Araki et al., 2000; Scott and Zhao, 2001). Therefore, we analyzed the roles of RAB3A and RAB11B in KCM-stimulated melanin exocytosis. For this, we silenced RAB11B or RAB3A in melanocytes cultured in RPMI, DMEM, or KCM with small interfering RNAs (siRNAs) and achieved ≥60% silencing (Figure 2a and b). A nontargeting siRNA was used as the negative control. We found that on RAB3A depletion, melanin exocytosis becomes impaired by 50% in melanocytes cultured in KCM but not in DMEM or RPMI (Figure 3a). We also observed that RAB11B silencing does not affect KCM-induced melanin exocytosis (Figure 3a). Instead, RAB11B silencing significantly reduces melanin exocytosis from melanocytes cultured in RPMI (Figure 3a), confirming our previous reports (Moreiras et al., 2019; Tarafder et al., 2014). To rule out the possibility that these differences are due to defects in melanin synthesis, which in turn can impair the amount of exocytosed melanin, we also analyzed the amount of intracellular melanin. We confirmed that the defects in melanin exocytosis are not mirrored by defects in melanin synthesis because no decrease in intracellular melanin was found in any of the conditions tested (Figure 3b). Rather, we observed a small but significant increase in intracellular melanin levels on RAB3A depletion in KCM-cultured melanocytes, which could be a consequence of the impairment in melanin exocytosis (Figure 3b).

To exclude the off-target effects of the siRNA pool used to silence RAB3A, we performed a rescue experiment. For this, we plated wild-type or lentivirus-transduced melan-ink4a melanocytes overexpressing GFP or human GFP RAB3A and then silenced these cells for RAB3A. RAB3A expression levels

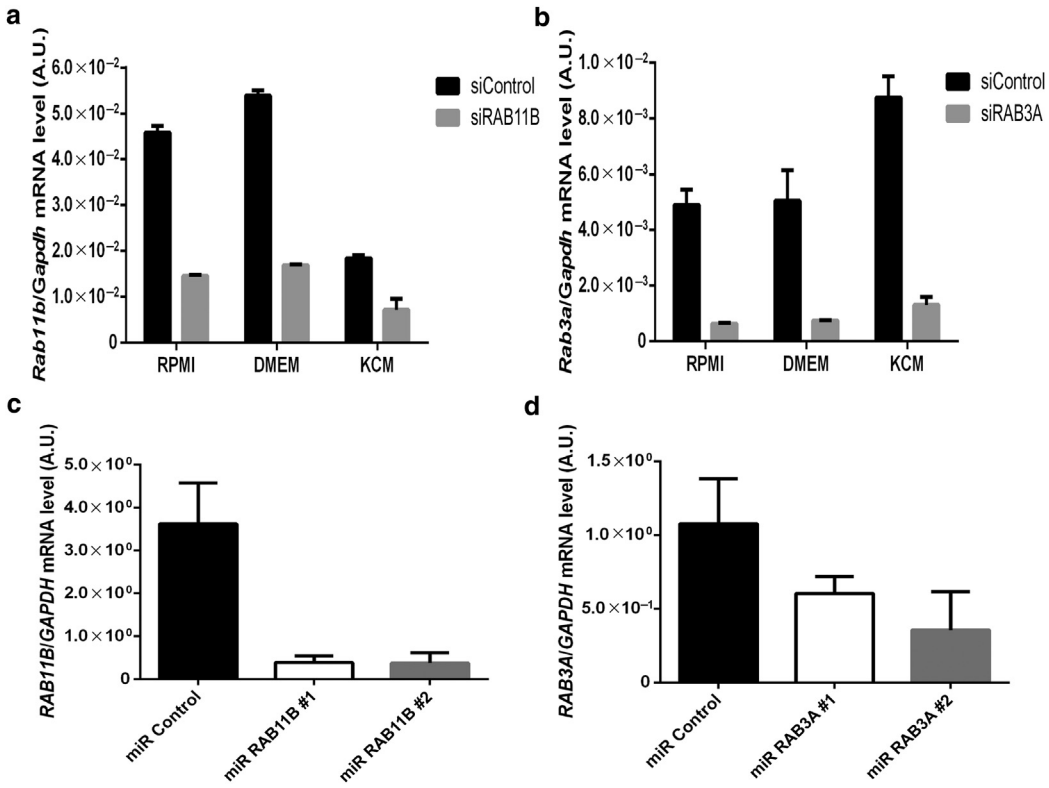

Figure 2. Silencing efficiency of *Rab11b/RAB11B* and *Rab3a/RAB3A* in melan-ink4a melanocytes and human neonatal epidermal darkly pigmented melanocytes. (**a**) *Rab11b* (siRAB11B) or (**b**) *Rab3a* (siRAB3A) silencing with siRNA smart pools in melan-ink4a melanocytes cultured in RPMI, DMEM, or KCM for 3 days. (**c**) *RAB11B* (miR RAB11B #1 and miR RAB11B #2) or (**d**) *RAB3A* (miR RAB3A #1 and miR RAB3A #2) silencing in human neonatal epidermal darkly pigmented melanocytes used for melanocyte/keratinocyte cocultures for 3 days. Plots show the values of relative mouse (*Rab3a* or *Rab11b*) or human (*RAB3A* or *RAB11B*) gene expression normalized to that of *Gapdh or GAPDH,* respectively. Error bars represent the mean ± SD of three independent experiments. #, number; A.U., arbitrary unit; KCM, keratinocyte-conditioned medium; siRab11b, Rab11b-targeted small interfering RNA; siRab3a, Rab3a-targeted small interfering RNA; siRNA, small interfering RNA.

were assessed by western blot to confirm the silencing and overexpression levels for all the conditions tested (Figure 4a and b). We found that by overexpressing GFP human RAB3A in RAB3A-silenced melanocytes, the amount of exocytosed melanin was restored to the levels observed in nontargeting siRNA melanocytes (Figure 3c). In addition, GFP RAB3A but not GFP overexpression can rescue the augmented intracellular melanin levels caused by RAB3A depletion (Figure 3d). Noteworthy, we found that KCM-stimulated melanocytes overexpressing GFP RAB3A show double the amount of exocytosed melanin compared with melanocytes overexpressing GFP (Figure 3e), whereas no significant differences in intracellular melanin were observed between the two conditions (Figure 3f). This reinforces the conclusion that RAB3A acts as a regulator of KCM-stimulated melanin exocytosis. Altogether, these results suggest the existence of two distinct melanin exocytosis pathways: a basal one regulated by RAB11B and another induced by KCM and regulated by RAB3A.

KCM enhances the recruitment of RAB3A to melanosomes in melanocyte dendrites

We next evaluated whether RAB3A colocalizes with melanosomes in melanocyte dendrites to regulate the final steps of melanosome fusion with the plasma membrane. To study this, we cultured melan-ink4a melanocytes in KCM or DMEM for 24 hours before fixing and immunolabeling with an anti-RAB3A antibody and an anti-TYRP1 antibody, which stains mature melanosomes (Benito-Martínez et al., 2020). First, we confirmed that endogenous RAB3A accumulates primarily in the perinuclear region, where it partially overlaps with the Golgi, as indicated by coat protein complex I labeling (Encarnação et al., 2016; Zerial and McBride, 2001) (Figure 5). We then evaluated the colocalization of RAB3A with TYRP1 in the dendrites of KCM-stimulated or DMEM-cultured melan-ink4a melanocytes. We found that the Mander's coefficient of colocalization between endogenous RAB3A and TYRP1-positive melanosomes in the dendrites of KCM-stimulated melanocytes (Figure 6a and c) was two times higher than that in DMEM-incubated melanocytes (Figure 6b and c). Because melanocyte dendrites are thin structures and could force the colocalization between RAB3A and melanosomes, we simultaneously quantified the colocalization between RAB3A and early endosome antigen 1 (EEA1) as a negative control. Similar Mander's coefficients of colocalization between endogenous RAB3A and EEA1-positive early endosomes were observed in both KCM-induced or DMEM-cultured melanocytes (Figure 6a, b, and d). Moreover, the absolute Mander's coefficient values for the RAB3A/EEA1 colocalization are close to the one observed for RAB3A/TYRP1 colocalization in DMEM-incubated melanocytes (Figure 6). Altogether, these results

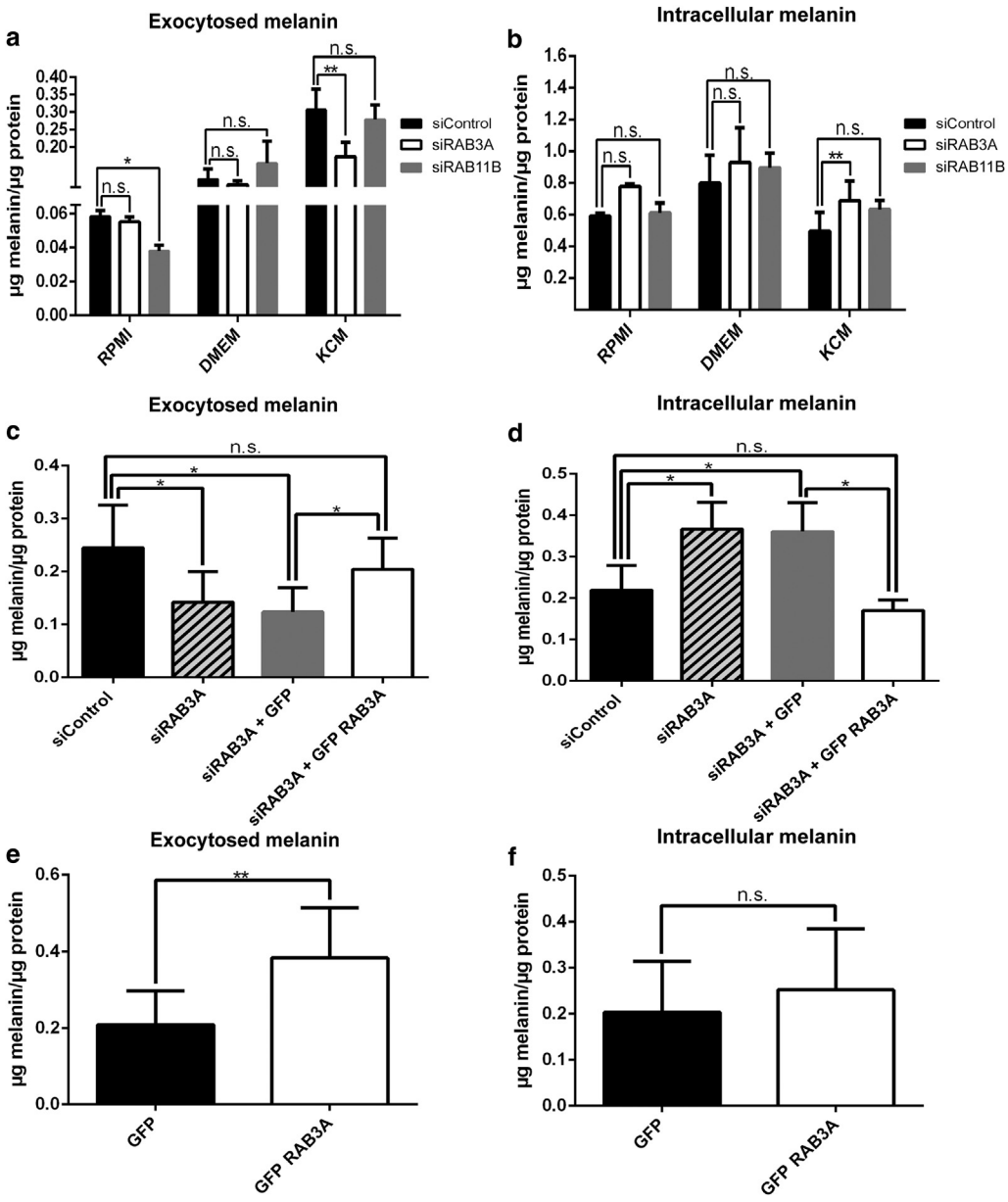

Figure 3. KCM induces melanin exocytosis in a RAB3A-dependent and RAB11B-independent manner. (**a**) Exocytosed and (**b**) intracellular melanin levels of melan-ink4a melanocytes cultured in RPMI, DMEM, or KCM and silenced for RAB3A (siRAB3A) or RAB11B (siRAB11B) or transfected with a siControl. (**c**) Exocytosed and (**d**) intracellular melanin levels of melan-ink4a melanocytes cultured in KCM overexpressing or not GFP or GFP human RAB3A and silenced for RAB3A or transfected with siControl. (**e**) Exocytosed and (**f**) intracellular melanin levels of melan-ink4a melanocytes cultured in KCM and overexpressing GFP or GFP human RAB3A. After 3 days of incubation with the indicated culture media, melanocyte melanin levels were quantified by fluorescence spectroscopy as described in the Materials and Methods. Melanin amounts (in µg) were normalized by total protein (in µg). The plots represent the mean ± SD of at least three independent experiments. Data were analyzed with (**a, b**) two-way ANOVA, (**c, d**) one-way ANOVA, or (**e, f**) two-tailed unpaired *t*-test. $*P < 0.05$ and $**P < 0.01$. KCM, keratinocyte-conditioned medium; n.s., nonsignificant; siControl, nontargeting small interfering RNA; siRAB11B, RAB11B-targeted small interfering RNA; siRAB3A, RAB3A-targeted small interfering RNA.

suggest that KCM stimulation increases the recruitment of RAB3A to melanosome membranes in melanocyte dendrites, where melanosome exocytosis predominantly occurs.

KCM from differentiated primary human KCs stimulates melanin exocytosis and transfer

To validate the results obtained with mouse cell lines in human primary cells, we started by differentiating human neonatal epidermal KCs (HEKns) by incubating with 2% fetal calf serum and 0.1 mM calcium, as described elsewhere (Borowiec et al., 2013). Importantly, we confirmed KC differentiation by immunofluorescence using antibodies for keratin 14 (a basal epidermal KC marker) and involucrin (a marker for spinous and granular epidermal KCs) (Borowiec et al., 2013). As expected, we observed that ~90% of differentiated HEKns express involucrin and do not express keratin 14, in contrast to ~90% of nondifferentiated HEKns that express keratin 14 and do not express involucrin (Figure 7). Interestingly, ~90% of XB2 mouse KCs express involucrin and not keratin 14, similar to differentiated HEKns (Figure 7). Then, we cultured human neonatal epidermal darkly pigmented melanocytes (HEMn-DPs) with primary KCM (pKCM) collected from nondifferentiated HEKns (nondifferentiated pKCM) or differentiated HEKns (differentiated pKCM) and assessed exocytosed melanin levels as well as intracellular melanin content. As controls, we cultured HEMn-DPs in DMEM-based primary FCM (pFCM) collected from human neonatal dermal fibroblasts or in nonconditioned DMEM. The results showed that HEMn-DPs incubated in differentiated pKCM exocytose twice more melanin than HEMn-DPs cultured in nondifferentiated pKCM (Figure 8a). Moreover, we observed a three-fold increase in melanin exocytosis from HEMn-DPs stimulated with differentiated pKCM compared with that from HEMn-DPs incubated with pFCM or DMEM (Figure 8a). No significant

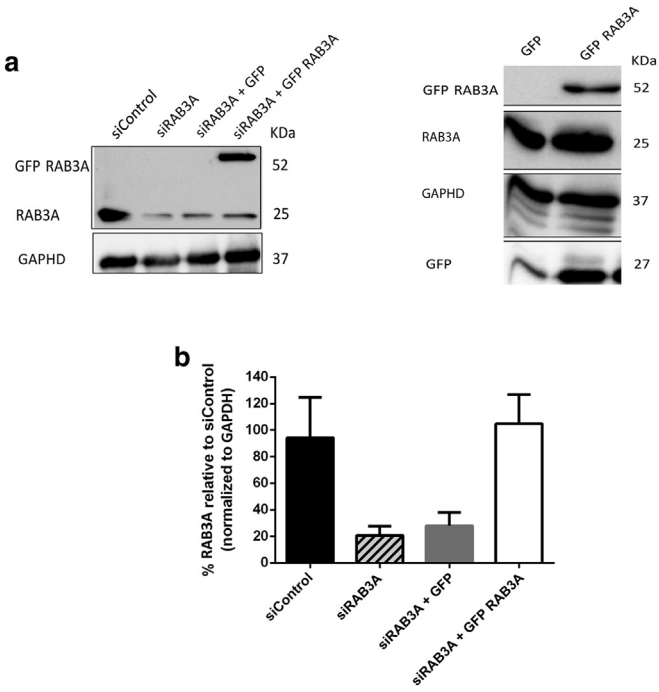

Figure 4. Silencing and rescue efficiency of RAB3A in melan-ink4a melanocytes. (**a**) Representative western blot for GFP human RAB3A, GFP, and endogenous RAB3A. GAPDH was used as a loading control. (**b**) Quantification of total RAB3A protein levels normalized to those of GAPDH and shown in percentage relative to the control. Protein extracts were obtained from melanocytes in culture with KCM for 3 days. Error bars represent the mean ± SD of three independent experiments. KCM, keratinocyte-conditioned medium; siControl, nontargeting small interfering RNA; siRab3a, RAB3A-targeted small interfering RNA.

differences were detected in intracellular melanin levels between the different media used (Figure 8b).

Finally, we tested whether differentiated pKCM also enhances melanin transfer in HEMn-DP/HEKn cocultures. To label melanin-containing compartments in KCs, which we proposed to be named melanokerasomes (Moreiras et al., 2021), an anti-HMB45 antibody was used to recognize the structural protein PMEL, as described by others (Benito-Martínez et al., 2020). By scoring the number of HMB45-positive melanokerasomes per KC, we observed that differentiated pKCM doubles the amount of melanin transferred to KCs compared with nondifferentiated pKCM (Figure 8c and d). Thus, using primary human cells, we confirmed the effect of KCM in stimulating melanin exocytosis and transfer and found that differentiated spinous/granular layer KCs but not nondifferentiated basal KCs can induce this effect.

KCM from differentiated primary human KCs stimulates melanin transfer in a RAB3A-dependent manner

To further investigate the regulation of stimulated melanin transfer with differentiated pKCM, we transduced HEMn-DPs with adenoviruses encoding miRNAs to silence RAB3A or RAB11B and achieved ≥50% silencing efficiency for RAB3A and ≥85% silencing efficiency for RAB11B (Figure 2c and d). Then, we used RAB3A- or RAB11B-silenced melanocytes to establish HEMn-DP/HEKn cocultures. As a control, we used HEMn-DPs transduced with adenoviruses encoding a nontargeting miRNA to perform the cocultures. After 3 days of culture in conditioned media, we fixed the cocultures and quantified melanin transfer by counting HMB45-positive melanokerasomes within KCs, as previously described (Benito-Martínez et al., 2020). For this, we looked for areas of the coverslips containing transduced HEMn-DPs, thus expressing GFP. RAB3A silencing with either one of the two miRNAs used causes impairment in melanin transfer of around 50% (Figure 9a and b). On the other hand, RAB11B silencing leads to a significant reduction in melanin transfer of around 20% (Figure 9a and b). Thus, these results further support a RAB3A-dependent KCM-stimulated melanin transfer.

DISCUSSION

Evidence for active and complex crosstalk between melanocytes and KCs in the epidermis is emerging. In this study, we report that KC-derived soluble factors stimulate melanin exocytosis from melanocytes, highlighting the importance of melanocyte–KC long-range communication in the regulation of pigmentation through melanin synthesis, transport, exocytosis, and transfer.

KCs are known to release extracellular vesicles carrying miRNAs, which in turn increase the expression of genes involved in melanogenesis and melanosome transport (Lo Cicero et al., 2015). However, in our system, we did not find a considerable activity of extracellular vesicles in stimulating melanin exocytosis because the fraction containing these did not show a significant effect in this process. Importantly, this exocytosis-stimulating activity is not present in conditioned media derived from melanocyte/KC cocultures. One possibility to explain the difference between MKCM and KCM is the consumption of soluble factors by the melanocytes in MKCM. Alternatively, KCs can downregulate the release of soluble factors upon internalizing the melanin secreted by melanocytes in a coculture context. In this case, KCs cultured alone would keep secreting factors to stimulate melanin synthesis and exocytosis in a positive feedback loop, resulting in a higher concentration of factors in the medium. Indeed, KCs alone or cocultured with melanocytes show a different secretome (Lo Cicero et al., 2015; Wäster et al., 2016). Furthermore, cocultures allow crosstalk mediated by cell-to-cell contacts, previously shown to regulate melanin synthesis and transfer (Belote and Simon, 2020; Domingues et al., 2020; Lo Cicero et al., 2015; Joshi et al., 2007; Wäster et al., 2016). Altogether, these results suggest that the crosstalk is mediated by both soluble factors and cell–cell contacts.

We also explored melanocyte–KC crosstalk in the regulation of melanin exocytosis and transfer in a more physiological context. Considering that melanocytes mainly contact with KCs from the basal layer of the epidermis rather than with differentiated spinous/granular KCs from the upper layers (Del Bino et al., 2018; Fitzpatrick and Breathnach, 1963), we evaluated whether human primary KC (HEKn) differentiation enhances the exocytosis-stimulating activity of the conditioned medium (pKCM, in this case). The results showed that pKCM collected from differentiated spinous/granular HEKns stimulates significantly more melanin exocytosis than pKCM collected from nondifferentiated basal HEKns. This is consistent with a model where exposure to UVR enhances the secretion of soluble factors by KCs from

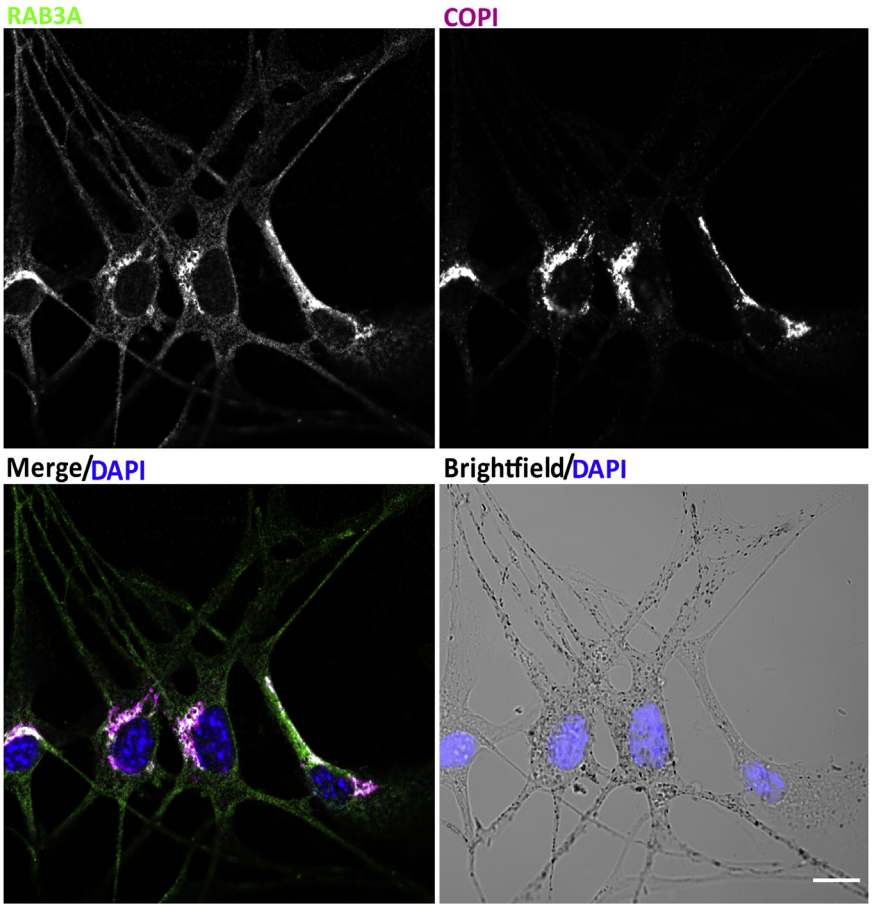

Figure 5. RAB3A accumulates primarily in the perinuclear region where it partially overlaps with the Golgi. Representative confocal images of melan-ink4a melanocytes coimmunostained for endogenous RAB3A (green) and the Golgi marker COPI (pseudocolored in magenta). Images were analyzed with ImageJ software. Melanocytes were stained with DAPI to label nuclei (blue), and the brightfield shows melanosomes as black dots. Bar = 10 μm. Images are representative of three independent experiments. COPI, coat protein complex I.

the upper layers of the epidermis, which in turn stimulates melanin synthesis (Hirobe, 2014; Taisuke and Hearing, 2011; Yamaguchi and Hearing, 2009) and transfer.

We next studied the molecular machinery regulating KCM-stimulated melanin exocytosis. Although we confirmed that RAB11B regulates melanin exocytosis from melanocytes cultured in RPMI, as previously reported by us (Moreiras et al., 2019; Tarafder et al., 2014), our results show that RAB3A instead regulates KCM-induced melanin exocytosis from melanocytes. Moreover, in KCM-stimulated cocultures, melanin transfer also occurs in a RAB3A-dependent manner. We also observed a small reduction in KCM-stimulated melanin transfer on RAB11B silencing, which is likely due to the coexistence of the basal route of transfer with the stimulated one in the cocultures incubated in KCM. Therefore, we suggest that long-range communication triggered by KCM soluble factors elicits RAB3A-mediated melanin exocytosis, whereas contact-mediated crosstalk occurring in non-KCM–stimulated two-dimensional cocultures elicits RAB11B-mediated melanin exocytosis (Figure 10). Further studies using three-dimensional reconstructed skin epidermis models irradiated or not with UVR should be performed to better understand the role of RAB11B and RAB3A in melanin transfer. In addition, it is possible that RAB3A-dependent melanin transfer occurs through other routes than exocytosis/phagocytosis (e.g., shedding vesicles) because this is a stimulated pathway (Moreiras et al., 2021).

Thus, our results suggest that melanocytes can coordinately regulate melanogenesis, melanosome peripheral transport, and regulated exocytosis. One such mechanism linking transport and exocytosis could involve a cooperative role in the actin-based transport regulated by RAB27A (Barral and Seabra, 2004; Hume et al., 2007; Wu et al., 2012) and exocytosis of melanosomes by RAB3A. Interestingly, such functional cooperation has been described for other lysosome-related organelles, including Weibel–Palade bodies and dense-core granules present in endothelial and sperm cells, respectively (Delevoye et al., 2019; Quevedo et al., 2019; Raposo et al., 2007; Zografou et al., 2012). Moreover, the exocytosis of sperm dense-core granules is regulated by RAB27A, RAB3A, and GRAB, a guanine nucleotide exchange factor recruited by RAB27A to activate RAB3A (Quevedo et al., 2019). Therefore, a cooperative RAB27A–RAB3A cascade could be involved in KCM-stimulated melanosome exocytosis and should be further investigated.

In summary, the emerging evidence is one of a complex crosstalk composed of short-range signals mediated by cell–cell contacts and long-range signals mediated by soluble factors, as shown in this study (Figure 10). Future studies should be directed at characterizing the KC-derived soluble factors present in KCM and identifying the signaling pathways upstream and downstream of RAB3A that promote melanin exocytosis from melanocytes.

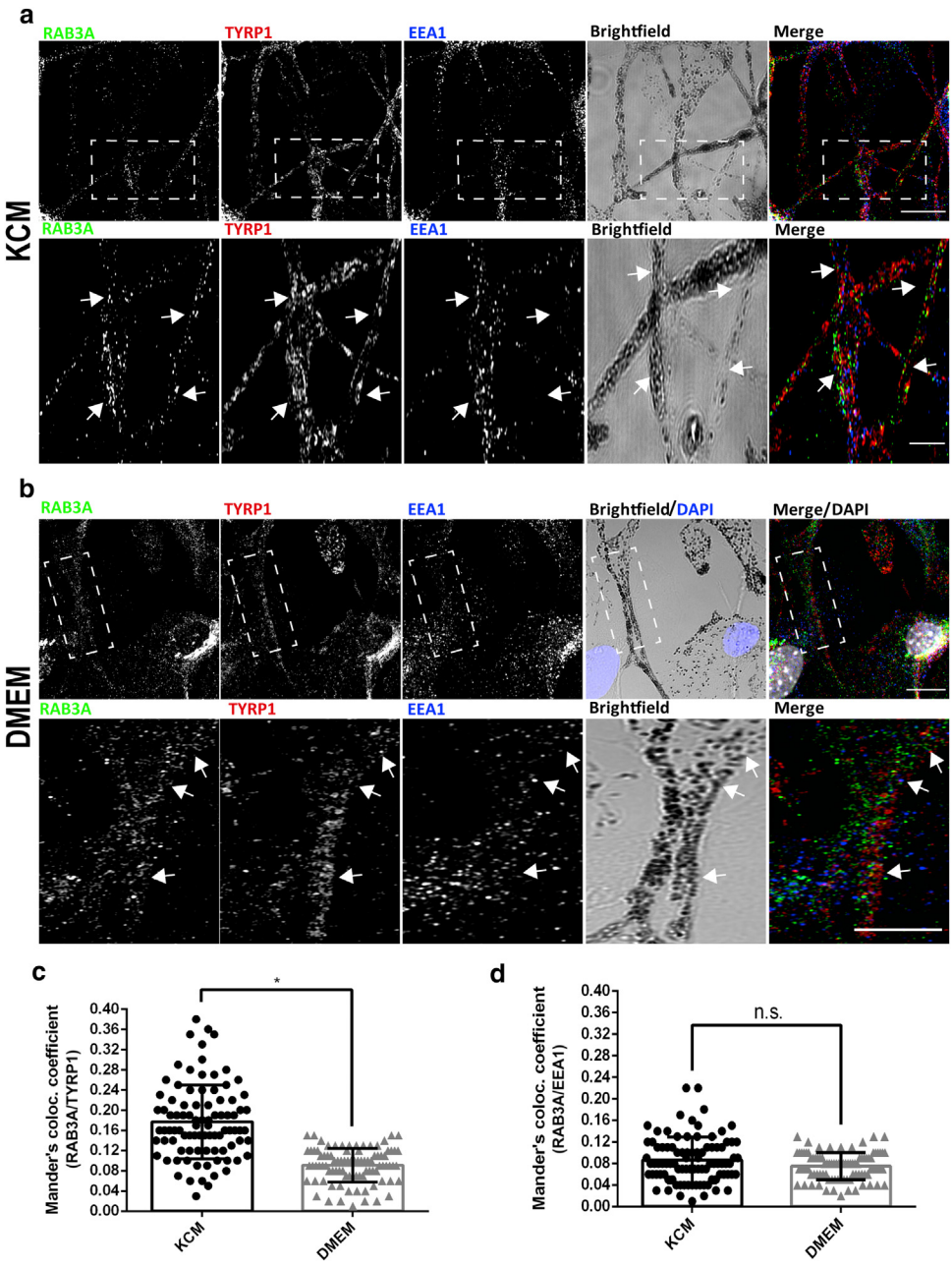

Figure 6. RAB3A recruitment to melanosomes is enhanced on stimulation with KCM. Confocal images of melan-ink4a melanocytes cultured in (**a**) KCM or (**b**) DMEM for 24 hours. Zoom-ins of dashed areas are shown in the lower panels. (**c**) Mander's coefficient of coloc. between TYRP1-positive melanosomes (in red) and endogenous RAB3A (in green) in melanocyte dendrites. (**d**) Mander's coefficient of coloc. between EEA1-positive early endosomes (pseudocolored in blue) and endogenous RAB3A (in green) in melanocyte dendrites. Brightfield shows melanosomes as black dots, and white arrows indicate RAB3A/TYRP1 colocalization. Cells were stained with DAPI to label nuclei (in blue for the brightfield panels or in gray for the merge panels). Bars = 10 μm (upper rows) and 5 μm (lower rows). The plot displays Mander's coefficient of colocalization in the melanocyte dendrites captured in 90 microscopy images per condition as mean ± SD of three independent experiments. Two-tailed unpaired *t*-test was applied to the mean values of each independent experiment in each condition. $*P < 0.05$. coloc., colocalization; KCM, keratinocyte-conditioned medium; n.s., nonsignificant.

MATERIALS AND METHODS

Mouse cell line culture

Melan-ink4a mouse melanocytes were cultured in RPMI-1640 (Gibco, Grand Island, NY) supplemented with 10% fetal bovine serum (FBS) (Gibco), 200 pM cholera toxin (Gentaur, Kampenhout, Belgium), 200 nM phorbol myristate acetate (Alfa Aesar, Heysham, United Kingdom), 100 units/ml penicillin (Gibco), and 100 μg/ml streptomycin (Gibco) at 37 °C with 10% carbon dioxide (CO_2). XB2 mouse KCs and mouse embryonic fibroblasts were cultured in DMEM (Gibco) supplemented with 10% FBS, GlutaMAX (2 mM L-alanyl-L-glutamine dipeptide, Gibco), 100 units/ml penicillin, and 100 μg/ml streptomycin at 37 °C with 10% CO_2 or 5% CO_2, respectively. Melan-ink4a/XB2 cocultures were incubated in DMEM supplemented with 10% FBS, GlutaMAX, 200 pM cholera toxin, 200 nM phorbol myristate acetate, 100 units/ml penicillin, and 100 μg/ml streptomycin at 37 °C with 10% CO_2. Both melan-ink4a and XB2 cells were obtained from the laboratory of Dorothy Bennett and Elena Sviderskaya (St. George's Hospital, London, United Kingdom) in June 2019, and on arrival, they were immediately used. Mouse embryonic fibroblasts were obtained from José Belo's group (NOVA Medical School, Universidade NOVA de Lisboa, Lisbon, Portugal). All the cell lines used were tested for mycoplasma using a PCR assay performed by the certified entity Eurofins Genomics Europe between July 2020 and July 2021.

Conditioned media production from mouse cell lines

To produce KCM, 10 ml of complete medium were added to XB2 KCs at 80% confluency and incubated for 3 days. In the case of FCM, mouse embryonic fibroblasts were incubated with 10 ml of complete medium for 3 days, starting at 60% confluency. Finally, to

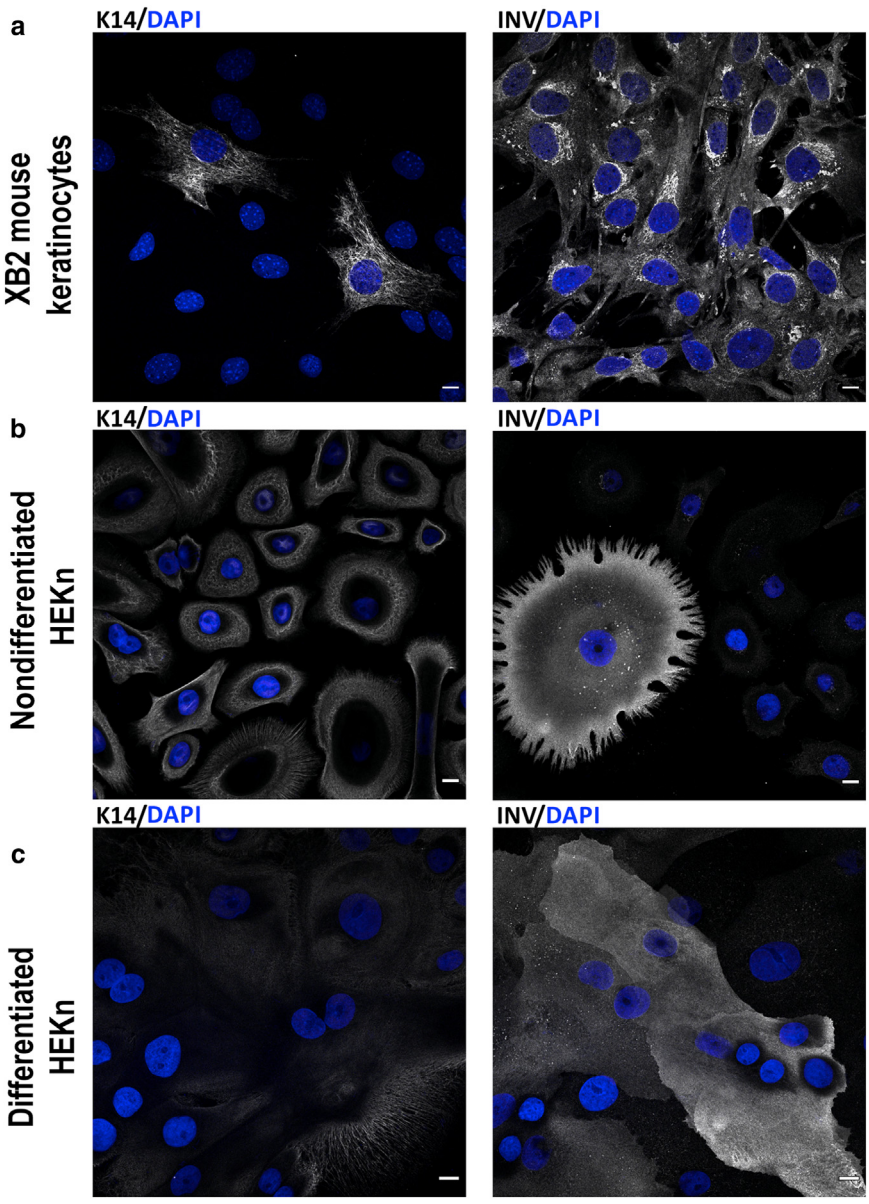

Figure 7. Differentiation staging of mouse XB2 keratinocytes cell line and human neonatal epidermal keratinocytes. Representative confocal images of (**a**) XB2 keratinocytes, (**b**) nondifferentiated HEKns, and (**c**) differentiated HEKns immunostained for K14 (left column) or INV (right column). Images were analyzed with ImageJ software. Cells were stained with DAPI to label nuclei (blue). Bars = 10 μm. Images are representative of three independent experiments. HEKn, human neonatal epidermal keratinocyte; INV, involucrin; K14, keratin 14.

produce MKCM, melan-ink4a melanocytes and XB2 KCs were seeded in 12-well plates in DMEM without cholera toxin or phorbol myristate acetate at a ratio of one melanocyte to five KCs. Then, the cocultures were incubated until they reached 80% confluency, and at that point, the culture medium was replaced by 2 ml of fresh DMEM medium and incubated for further 3 days. After collection, all conditioned media were filtered using a 0.45 μm syringe filter (Sarstedt, Nümbrecht, Germany) and stored at −80 °C until they were used. MKCM was centrifuged at 21,000*g* for 1.5 hours at 4 °C to discard exocytosed melanin before being stored. Finally, to fractionate KCM and MKCM, we subjected these media to ultracentrifugation at 100,000*g* for 2 hours at 4 °C and collected the supernatant (S100 fraction). The pellets containing extracellular vesicles (P100 fraction) were resuspended in DMEM.

Primary human cell culture

HEMn-DPs (C-202-5C, Gibco) were cultured in 254 medium (M-254-500, Gibco) with human melanocyte growth supplement (S-002-5, Gibco), 100 units/ml penicillin (Gibco), and 100 μg/ml streptomycin (Gibco). HEKns (C-020-5C, Gibco) were cultured in EpiLife medium (M-EPIcf-500, Gibco) with human KC growth supplement (S-001-5, Gibco), 0.06 mM calcium chloride, 100 units/ml penicillin (Gibco), and 100 μg/ml streptomycin (Gibco). Finally, human neonatal dermal fibroblasts (C-004-5C, Gibco) were cultured in DMEM (Gibco) supplemented with 10% FBS, GlutaMAX (2 mM L-alanyl-L-glutamine dipeptide, Gibco), 100 units/ml penicillin, and 100 μg/ml streptomycin. HEMn-DPs, HEKns, and human neonatal dermal fibroblasts were grown at 37 °C with 5% CO_2. All commercial human neonatal cells were derived from tissues obtained from accredited institutions, including tissue and organ procurement organizations, qualified research tissue organizations, and prominent academic and medical centers, through collaborations that follow rigorous regulations, certifications, and/or accreditations. Tissues obtained through these source facilities, which are under nondisclosure agreements, are consistent with the legal and ethical practices of the United States and the European Union, following the United States federal guidance on the use of human subjects in research (45 CFR part 46, subparts A, B, C, and D); the Health

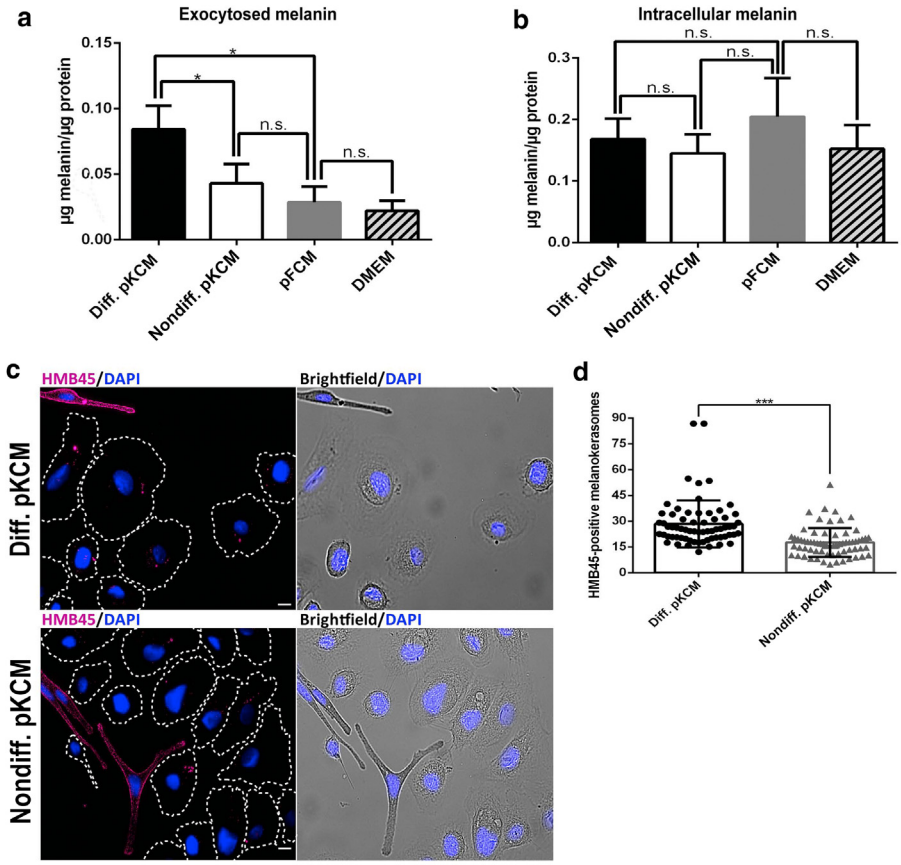

Figure 8. Melanin exocytosis and transfer are stimulated by keratinocyte-conditioned medium from differentiated primary human keratinocytes. (**a**) Exocytosed and (**b**) intracellular melanin levels of HEMn-DPs cultured in DMEM for 3 days, pKCM collected from differentiated HEKns (differentiated pKCM), or nondifferentiated HEKns (nondifferentiated pKCM) or primary FCM collected from human neonatal dermal fibroblasts. Exocytosed and intracellular melanin levels were quantified by fluorescence spectroscopy as described in the Materials and Methods. Melanin amounts (in µg) were normalized for the total protein (also in µg). (**c**) Representative microscopy images of HEMn-DP/HEKn cocultures incubated with differentiated pKCM or nondifferentiated pKCM for 3 days. Melanin-containing compartments inside keratinocytes, that is, melanokerasomes, were immunolabelled with anti-HMB45 antibody (pseudocolored in magenta) and shown as black dots in the brightfield. Cells were stained with DAPI to label nuclei (blue), and HEKn boundaries were outlined with white dashed lines. Bars = 10 µm. (**d**) Quantification of melanin transfer displayed as the number of HMB45-positive melanokerasomes per keratinocyte. HMB45 puncta were counted using the spot detector plugin in the Icy 2.0.2.0 software. A total of 70 different images per condition were acquired, and the number of HMB45-positive melanokerasomes per HEKn was plotted. All the plots represent the mean ± SD of at least three independent experiments. (**a, b**) One-way ANOVA or (**d**) two-tailed unpaired *t*-test were applied to the mean values of each independent experiment in each condition. $*P < 0.05$ and $***P < 0.0001$. Diff., differentiated; HEKn, human neonatal epidermal keratinocyte; HEMn-DP, human neonatal epidermal darkly pigmented melanocyte; Non-diff., nondifferentiated; n.s., nonsignificant; primary FCM, primary fibroblast-conditioned medium; pKCM, primary keratinocyte-conditioned medium.

Insurance Portability and Accountability Act, which addresses issues of confidentiality of personal information; the National Organ Transplant Act (42 CFR part 482); and the Uniform Anatomical Gift Act of 1968, revised in 1984. Written informed consent was obtained by these institutions from the donor or the donor's legal next of kin for use of the tissue and its derivatives for research purposes.

Human KC differentiation

Glass coverslips in 12-well plates were coated with bovine collagen I diluted 1:1,000 (A1064401, Gibco), and then HEKns were plated at 3×10^5 cells/well in supplemented EpiLife medium. On the following day, the medium was changed to EpiLife with 2% fetal calf serum (12105, Sigma-Aldrich, Steinheim, Germany) and 0.1 mM calcium chloride to start differentiation, as described elsewhere (Borowiec et al., 2013). As a negative control, HEKns were maintained in supplemented EpiLife (without fetal calf serum or calcium). The cells were differentiated for 24 hours, and their differentiation stage was confirmed by immunofluorescence analysis.

Conditioned media production from primary human cells

After differentiation, HEKn culture medium was changed to EpiLife with 2% fetal calf serum, and pKCM from differentiated HEKns (differentiated pKCM) or nondifferentiated HEKns (nondifferentiated pKCM) were collected after 3 days. Human neonatal dermal fibroblasts were plated at 5×10^5 cells/well in six-well plates in DMEM medium, and on the following day, the culture medium was renewed. Primary FCM (pFCM) was collected after 3 days. All conditioned media were filtered using a 0.45 µm syringe filter (Sarstedt) and stored at −80 °C until they were used.

siRNA transfection

Melan-ink4a melanocytes were cultured at 8.5×10^4 cells/well in 12-well plates. Whereas 50 nM of SMART pool siRNAs (Thermo Fisher Scientific, Lenexa, Kansas) (Table 1) were added to 250 µl of Opti-MEM (Gibco), 2.5 µl of DharmaFECT 4 (Dharmacon, Lafayette, Colorado) were added to 250 µl of Opti-MEM. After 5 minutes of incubation at room temperature, the two mixtures were combined, mixed gently, and incubated for 20 minutes at the same temperature.

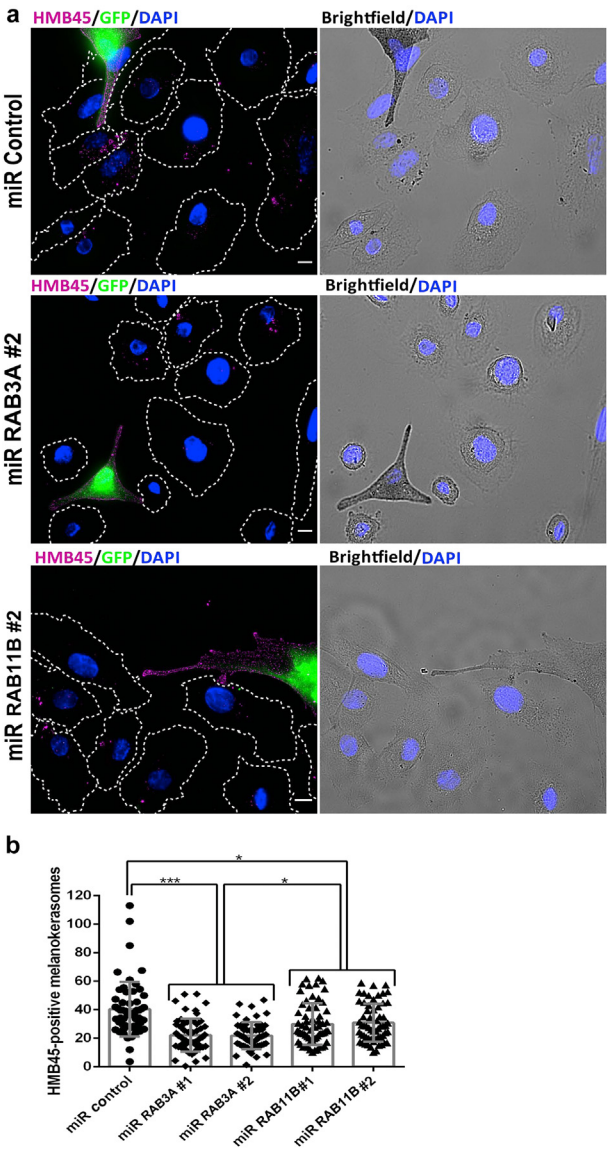

Figure 9. Keratinocyte-conditioned medium from differentiated primary human keratinocytes stimulates melanin transfer in a RAB3A-dependent manner. Before performing HEMn-DP/HEKn cocultures, HEMn-DPs were transduced with nontargeting miRNA (miR control) or miRNAs targeting RAB3A (miR RAB3A number 1 or miR RAB3A number 2) or RAB11B (miR RAB11B number 1 or miR RAB11B number 2). (**a**) Representative microscopy images of control and one miR for each silenced protein of HEMn-DP/HEKn cocultures stimulated with differentiated pKCM for 3 days, showing transduced HEMn-DPs in green (GFP) and melanin-containing compartments immunolabeled with HMB45 (pseudocolored in magenta). Melanin is shown as black dots in the brightfield. Cells were stained with DAPI to label nuclei (blue), and HEKn boundaries were outlined with white dashed lines. Bars = 10 μm. (**b**) Quantification of melanin transfer displayed as the number of HMB45-positive melanokerasomes per keratinocyte. A total of 60 coculture images containing five or more keratinocytes were acquired, and HMB45-positive puncta were counted using the spot detector plugin in the Icy 2.0.2.0 software. Results represent the mean ± SD of three independent experiments. One-way ANOVA was applied to the mean values of each independent experiment in each condition. $*P < 0.05$ and $***P < 0.0001$. #, number; HEKn, human neonatal epidermal keratinocyte; HEMn-DP, human neonatal epidermal darkly pigmented melanocyte; miRNA, microRNA; pKCM, primary keratinocyte-conditioned medium.

The growth medium from cells seeded the day before transfection was removed and replaced by the siRNA mixture in a total volume of 500 μl in Opti-MEM. Cells were incubated for 24 hours at 37 °C, and then the medium was changed to 1 ml of complete RPMI, DMEM, or KCM supplemented with 200 pM cholera toxin and 200 nM phorbol myristate acetate. After 3 days, cells were assayed, and silencing efficiency was confirmed by qPCR.

Viral production and cell transduction

The lentiviral vector pLenti6/V5-DEST Gateway was used to achieve stable overexpression of GFP or GFP human RAB3A. For this, the cDNA sequences were inserted into the lentiviral vector. For lentivirus production, STAR-RDpro cells grown in DMEM supplemented with 10% FBS, 2 mM GlutaMAX, and 15 mM N-2-hydroxyethylpiperazine-N′-2-ethanesulfonic acid were cotransfected using jetPRIME (Poly Plus, Berkeley, CA) with 2.5 μg of lentiviral vector, 3.5 μg packaging plasmid (pxPAX2), and 1.8 μg envelope plasmid (pCMV-VSV-G). Media containing lentiviral particles were harvested 48 hours after transfection and stored in aliquots at −80 °C until use. Melan-ink4a cells were plated at 8.5×10^4 cells/well in 12-well plates and transduced on the next day with approximately 3×10^5 plaque-forming units of lentiviral particles in the presence of 8 μg/ml polybrene (hexadimethrine bromide, Sigma-Aldrich). After 24 hours, 9 μg/ml of blasticidin were added to transduced cells. Cells were selected for at least 5 days before being assayed.

Adenoviruses were produced according to the ViraPower Invitrogen protocol (https://www.thermofisher.com/pt/en/home/references/protocols/proteins-expression-isolation-and-analysis/adenovirus-protocol/virapower-adenoviral-expression-system.html). miRNA sequences for RAB3A and RAB11B and the nontargeting miRNA sequence (negative control) are described in Table 2. HEMn-DPs were plated at 7.5×10^4 cells/well on 12-well plates and transduced on the next day with 3×10^5 plaque-forming units of adenoviral particles.

qPCR quantification of gene expression

Total RNA was isolated from cells using the RNeasy Mini kit (Qiagen, Venlo, Netherlands) and converted to cDNA using SuperScript II (Invitrogen, Lenexa, Kansas) according to the manufacturers' instructions. qPCR reactions were performed using a Roche LightCycler (Roche, Grenzacherstrasse, Switzerland) and Roche SybrGreen Master Mix reagent (SybrGreen, Roche) according to the manufacturer's instructions. For each gene, specific primers were used (Table 3). Mouse or human gene expression was calculated relative to that of the control cells and normalized to *Gapdh* or *GAPDH*, respectively.

Immunofluorescence microscopy

Coverslips containing cells were washed three times with PBS, and cells were fixed with 4% paraformaldehyde (Alfa Aesar) in PBS for 20 minutes. Blocking and permeabilization were done by incubating the cells for 1 hour with Perblock solution (1% FBS, 0.5% BSA, and 0.1% Saponin in PBS). Coverslips were then incubated with primary antibodies (Table 4) for 2 hours in a humidified chamber. After washing three times with PBS, coverslips were incubated with respective Alexa secondary antibodies, avoiding species cross-reaction (Table 4), for 1 hour in a humidified chamber. Finally, coverslips were washed three times with PBS and mounted with Fluoromount-G with DAPI (Invitrogen) to visualize the cells' nuclei. All the steps were performed at

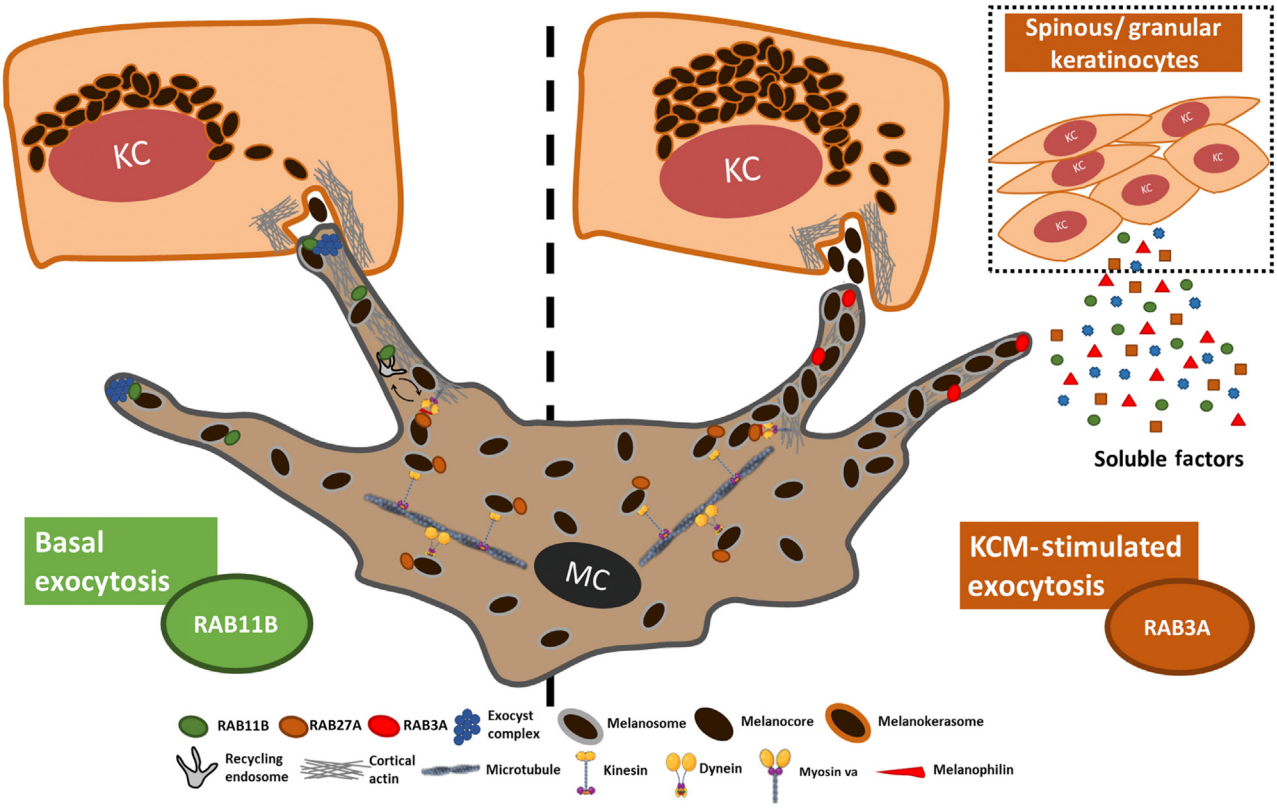

Figure 10. Schematic representation of melanin exocytosis pathways in melanocytes. Melanosomes are tethered to the cortical actin through the tripartite complex RAB27A/melanophilin/myosin Va. Melanosomes can then undergo a basal exocytosis pathway or a KCM-stimulated one. In the former (left), RAB11B-positive recycling endosomes are postulated to remodel melanosome membranes, which then interact with the exocyst before being exocytosed as melanocores from the dendrites of melanocytes. Then, keratinocytes internalize and store the melanocores in specialized organelles, which we proposed to name melanokerasomes. Alternatively, melanin exocytosis can be triggered by KCM-soluble factors released by spinous/granular keratinocytes (right). This KCM-stimulated route is characterized by higher melanin exocytosis and transfer rate and is regulated by RAB3A. KC, keratinocyte; KCM, keratinocyte-conditioned medium.

room temperature. The images were acquired in a Zeiss LSM 980 Airyscan confocal microscope or with a ZEISS Axio Imager 2 microscope with a PlanApochromat 63 × 1.4 numerical aperture oil-immersion objective and analyzed with ImageJ software (National Institutes of Health, Bethesda, MD) (Schindelin et al., 2012) or Icy 2.0.2.0 software (De Chaumont et al., 2012).

Colocalization analysis

Melan-ink4a melanocytes were seeded on glass coverslips in 24-well plates (3×10^4 cells/well) and incubated with KCM or DMEM for 24 hours. Then, cells were fixed and processed for immunofluorescence microscopy by incubating with an anti-RAB3A antibody and an anti-TYRP1 antibody (Table 4). For colocalization analysis, microscopy images were acquired in a Zeiss LSM 980 Airyscan confocal microscope, and Mander's coefficient was calculated by using spot detector (Olivo-Marin, 2002) and colocalization studio (Lagache et al., 2015) plugins in Icy 2.0.2.0 software (De Chaumont et al., 2012). ImageJ software (Schindelin et al., 2012) was used to adjust image brightness and contrast and do the merging.

Immunoblotting

Melan-ink4a melanocytes plated on 12-well plates and transfected/transduced with siRNAs and/or lentiviruses were lysed in ice-cold lysis buffer (50 mM Tris-hydrogen chloride, pH 7.5, 150 mM sodium chloride, 1 mM EDTA, 1 mM EGTA, 2 mM magnesium chloride, 1 mM dithiothreitol, and 1% IGEPAL) in the presence of protease inhibitors for 30 minutes on ice, followed by centrifugation at 21,000*g* for 30 minutes at 4 °C. Total protein concentration was quantified using the detergent-compatible protein assay kit (Bio-Rad Laboratories, Hercules, CA), following the manufacturer's protocol, and equal protein amounts per sample were resuspended in a 2× loading buffer. Then, samples were resolved on 12% SDS-PAGE, and the protein bands were transferred onto activated nitrocellulose membranes at 100 V in transfer buffer (25 mM Tris, 192 mM glycine,

Table 1. List of SMART Pool siRNAs Used

siRNAs	Species	Sequences (5′–3′)
RAB3A	Mouse	CCACUCAGAUCAAAACUUA
		UGUCAGCACCGUUGGCAUA
		GGACGUGAUCUGUGAGAAG
		CCAUCUACCGCAACGACAA
RAB11B	Mouse	ACAGAAAUCUACCGUAUUG
		CGAGUACGAUUACCUAUUC
		GCAGAUAGCAACAUUGUCA
		GUGCACUGCUGGUAUAUGA
Control	Mouse	GAAGAUAUCGUCCGCAUUA
		GUUGAAAUUUGACCAGUUA
		GAACUUAGCAGGAGAGAGU
		CUUCAGAUGUGUUCAAGAA

Abbreviation: siRNA, small interfering RNA.

Table 2. List of miRNAs Used

miRNA	Species	Sequence (5′–3′)
Control	Human	TACTGCGCGTGGAGACGTTTT
RAB3A #1	Human	TGACCTTGAAGTCTATGCCAA
RAB3A #2	Human	AACATATAGTCGAAGTTCTGG
RAB11B #1	Human	TGAGGATGTTCTTGAATGCTT
RAB11B #2	Human	AGGTAATCGTACTCGTCGTC

Abbreviations: #, number; miRNA, microRNA.

and 20% ethanol) for 55 minutes at room temperature. Membranes were blocked with blocking buffer (5% nonfat dry milk and 0.1% Tween-20 in PBS) and incubated with the primary polyclonal antibodies goat anti-RAB3A and anti-GAPDH (Table 4). All primary antibodies were separately incubated overnight at 4 °C under constant mixing. After each incubation, membranes were washed three times with PBS + 0,1% Tween-20 and incubated for 1 hour at room temperature with horseradish peroxidase–conjugated secondary anti-goat antibody (Table 4). Antibody complexes were visualized by employing the enhanced chemiluminescence reagent (Amersham Biosciences, Waukesha, WI). The signal was detected using an Imager Chemidoc XRS (Bio-Rad Laboratories), and the images were preprocessed with Image Lab software (Bio-Rad Laboratories). Band intensities were quantified using ImageJ software (Schindelin et al., 2012) by generating peaky histograms that are proportional to the area and intensity of bands. The housekeeping protein GAPDH was used to normalize RAB3A levels, and the results were indicated as percentages relative to control. Finally, membrane stripping was done by incubating twice with a mild stripping buffer (1.5% glycine, 0.1% SDS, and 1% Tween, pH 2.2) for 5 minutes at room temperature. Stripped membranes were then incubated with primary polyclonal antibody goat anti-GFP (Table 4), followed by horseradish peroxidase–conjugated secondary anti-goat, and developed as described earlier.

Melanin quantification

Wild-type melan-ink4a melanocytes or lentivirus-transduced melan-ink4a melanocytes overexpressing GFP or GFP human RAB3A were seeded in 12-well plates at 8.5 × 10^4 cells/well. On the next day, melanocytes were silenced using SMART pool siRNAs (Table 1). Then, cells were incubated with RPMI, DMEM, or KCM supplemented with 200 pM cholera toxin and 200 nM phorbol myristate acetate. In the case of HEMn-DPs, cells were seeded in 12-well plates at 1 × 10^5 cells/well and then incubated with differentiated pKCM, nondifferentiated pKCM, pFCM, or DMEM. After 3 days, the culture medium was collected and centrifuged at 300*g* for 5 minutes to remove dead cells. The supernatant was collected and centrifuged at 21,000*g* at 4 °C for 1.5 hours to precipitate melanin. Afterward, the pellet was resuspended in 90 μl of sodium hydroxide 1 M (LabKem, Migjorn, Barcelona) with 10% DMSO (Sigma-Aldrich).

To quantify intracellular melanin, cells were trypsinized and collected by centrifugation at 300*g* for 5 minutes. The pellet obtained was washed with PBS, centrifuged again at 300*g* for 5 minutes, and then lysed in 500 μl of 1 M sodium hydroxide + 10% DMSO. Melanin samples, including synthetic melanin (Sigma-Aldrich) to obtain the standard curve, were solubilized in 1 M sodium hydroxide + 10% DMSO, boiled at 80 °C for 1 hour, and centrifuged at 3,000*g* for 5 minutes to remove insoluble debris. Then, 50% (w/v) hydrogen peroxide (Acros Organics, Lenexa, Kansas) was added to all the samples to a final concentration of 30% (v/v) and incubated for 4 hours at room temperature in the dark. Finally, 200 μl of the sample were added to black opaque 96-well plates (Greiner, Kremsmünster, Austria) and read in a SpectraMax i3x multimode microplate reader (FortéBio, Goettingen, Germany) using an optimized reading distance of 2.81 mm and excitation/emission wavelengths of 470 nm/550 nm. The amount of melanin for each sample was normalized to the total protein. For this, the protein content in the cell lysates was measured at 562 nm in the same plate reader using the Pierce BCA protein kit (Thermo Fisher Scientific) and following the manufacturer's instructions. Exocytosed and intracellular melanin amounts were calculated by interpolating their fluorescence values with the ones from the standard curve of synthetic melanin, considering 1 M sodium hydroxide + 10% DMSO as blank and normalizing to the protein levels of each sample.

Table 3. List of Primers Used

Primers	Species	Sequences (5′–3′)
Rab3a forward	Mouse	TTAATGCAGTGCAGGACTGG
Rab3a reverse		CAGGCACAATCCTGATGAGG
Rab11b forward	Mouse	AAGGAGCTGCGGGATCATGC
Rab11b reverse		ACAGGCTCTGGCAGCACTGC
Gapdh forward	Mouse	AACTTTGGCATTGTGGAAG
Gapdh reverse		ACACATTGGGGGTAGGAAC
RAB3A forward	Human	GAGTCCTCGGATCAGAACTTCG
RAB3A reverse		TGTCGTTGCGATAGATGGTCT
RAB11B forward	Human	TCACCCGCAACGAGTTCAAC
RAB11B reverse		CTGCACCACGGTAGTACGC
GAPDH forward	Human	CATTTCCTGGTATGACAACGA
GAPDH reverse		GTCTACATGGCAACTGTGAG

Melanin transfer assay in primary human melanocyte/KC cocultures

HEMn-DPs were plated at 12-well plates and transduced with adenoviruses encoding miRNAs targeting RAB3A or RAB11B or non-targeting miRNA (negative control) (Table 2), as described earlier. On the following day, HEMn-DPs were detached and reseeded (2 × 10^4 cells/well) with HEKns (1 × 10^5 cells/well) at a ratio of 1:6 in 24-well plates containing glass coverslips previously coated with bovine collagen I diluted 1:1,000 (A1064401, Gibco). After 3 days, the coverslips were fixed and incubated with anti-HMB45 antibody (Table 4) to label melanin and mounted, following the protocol described earlier. Finally, the images were acquired in a ZEISS Axio Imager 2 microscope with a PlanApochromat 63 × 1.4 numerical aperture oil-immersion objective. To quantify melanin transfer, HMB45-positive melanin-containing organelles present within KCs, which we proposed to call melanokerasomes (Moreiras et al., 2021), were counted using the spot detector plugin (Olivo-Marin, 2002) in the Icy 2.0.2.0 software (De Chaumont et al., 2012) and normalized to the number of HEKns analyzed in each image.

Statistical analysis

All numerical data are representative of three or more biological replicates and presented as mean ± SD. One-way ANOVA (Dunnett's multiple comparison test) was used to compare different datasets with controls, except for the comparison between miR RAB11B and miR RAB3A (Figure 9). In this case, one-way ANOVA (Tukey's multiple comparison test) was used. In experiments with more than one control, one-way ANOVA (Tukey's multiple comparisons test) or two-way ANOVA (Tukey's multiple comparisons

Table 4. List of Antibodies Used

Antibodies	Raised in Species	Brand and Reference	Western Blot Dilution	Immunofluorescence Dilution
Anti-RAB3A	Goat	SICGEN (AB0032-100)	1:1,000 in PBS	1:200 in PBS
Anti-TYRP1	Mouse	Abcam (ab190709)	Not applicable	1:1,500 in PBS
Anti-HMB45	Mouse	Dako (M0634)	Not applicable	1:200 in Perblock solution
Anti-COPI	Mouse	Hybridoma clone M3A5	Not applicable	1:200 in Perblock solution
Anti−keratin14	Mouse	Abcam (ab9220)	Not applicable	1:1,000 in Perblock solution
Anti-involucrin	Mouse	Abcam (ab68)	Not applicable	1:200 in Perblock solution
Anti-GAPDH	Goat	SICGEN (AB0049-500)	1:1,000 in blocking buffer	Not applicable
Anti-GFP	Goat	SICGEN (AB0020-200)	1:1,000 in blocking buffer	Not applicable
HRP-conjugated secondary anti-goat antibody	Donkey	Thermo Fisher Scientific (A16005)	1:7,000 in blocking buffer	Not applicable
Alexa 568−conjugated anti-mouse secondary antibody	Goat	Thermo Fisher Scientific (A11004)	Not applicable	1:500 in Perblock solution
Alexa 555−conjugated anti-mouse secondary antibody	Donkey	Thermo Fisher Scientific (A32773)	Not applicable	1:500 in Perblock solution
Alexa 488−conjugated anti-goat secondary antibody	Donkey	Thermo Fisher Scientific (A11055)	Not applicable	1:500 in Perblock

Abbreviations: COPI, coat protein complex I; HRP, horseradish peroxidase;

test) were applied to data with one independent variable or two independent variables, respectively. Two-tailed unpaired *t*-test with Welch's correction was applied to the plots showing two conditions with only one independent variable. The statistical analyses were performed using GraphPad Prism software, version 6.01 (GraphPad Software, San Diego, CA).

Data availability statement

No datasets were generated or analyzed during this study.

ORCIDs

Luís C. Cabaço: http://orcid.org/0000-0003-0976-1781
Liliana Bento-Lopes: http://orcid.org/0000-0002-6893-610X
Matilde V. Neto: http://orcid.org/0000-0003-2267-6397
Andreia Ferreira: http://orcid.org/0000-0003-0657-354X
Wanja B. L. Staubli: http://orcid.org/0000-0001-7765-7260
José S. Ramalho: http://orcid.org/0000-0002-1927-164X
Miguel C. Seabra: http://orcid.org/0000-0002-6404-4892
Duarte C. Barral: http://orcid.org/0000-0001-8867-2407

AUTHOR CONTRIBUTIONS

Conceptualization: LCC, LBL, MCS, DCB; Formal Analysis: LCC, DCB; Funding Acquisition: DCB; Investigation: LCC, LBL, MVN, AF, WBLS, MCS, DCB; Methodology: LCC, LBL, MVN, AF, WBLS; JSR, MCS; DCB; Project Administration: DCB; Resources: JSR, MCS, DCB; Supervision: MCS, DCB; Validation: LCC, DCB; Visualization: LCC, DCB; Writing - Original Draft Preparation: LCC, LBL, MCS, DCB; Writing − Review and Editing: LCC, DCB

CONFLICT OF INTEREST

The authors state no conflict of interest.

ACKNOWLEDGMENTS

We would like to thank our group for the critical reading of the manuscript and the NMS microscopy and cell culture facilities, as well as José Belo's group, for the kind gift of mouse embryonic fibroblasts. This study was supported by Fundação para a Ciência e a Tecnologia (Portugal) through grant PTDC/BIA-CEL/29765/2017 and PhD fellowships to LCC, MVN, LBL and AF (2020.08812.BD, PD/BD/137442/2018, SFRH/BD/131938/2017 and PD/BD/135506/2018, respectively). This work was developed with the support from the research infrastructure PPBI-POCI-01-0145-FEDER-022122, cofinanced by Fundação para a Ciência e a Tecnologia (Portugal) and Lisboa2020, under the PORTUGAL2020 agreement (European Regional Development Fund). This article was supported by the LYSOCIL project, which has received funding from the European Union's Horizon 2020 research and innovation program under grant agreement number 811087. This work was also supported by iNOVA4Health − UIDB/04462/2020 and UIDP/04462/2020 and by the Associated Laboratory LS4FUTURE (LA/P/0087/2020), two programs financially supported by Fundação para a Ciência e a Tecnologia/Ministério da Ciência, Tecnologia e Ensino Superior (Portugal).

REFERENCES

Araki K, Horikawa T, Chakraborty AK, Nakagawa K, Itoh H, Oka M, et al. Small GTPase Rab3A is associated with melanosomes in melanoma cells. Pigment Cell Res 2000;13:332−6.

Barral DC, Seabra MC. The melanosome as a model to study organelle motility in mammals. Pigment Cell Res 2004;17:111−8.

Belote RL, Simon SM. Ca2+ transients in melanocyte dendrites and dendritic spine-like structures evoked by cell-to-cell signaling. J Cell Biol 2020;219:e201902014.

Benito-Martínez S, Zhu Y, Jani RA, Harper DC, Marks MS, Delevoye C. Research techniques made simple: cell biology methods for the analysis of pigmentation. J Invest Dermatol 2020;140:257−68.e8.

Borowiec AS, Delcourt P, Dewailly E, Bidaux G. Optimal differentiation of in vitro keratinocytes requires multifactorial external control. PLoS One 2013;8:e77507.

De Chaumont F, Dallongeville S, Chenouard N, Hervé N, Pop S, Provoost T, et al. Icy: an open BioImage informatics platform for extended reproducible research. Nat Methods 2012;9:690−6.

Del Bino S, Duval C, Bernerd F. Clinical and biological characterization of skin pigmentation diversity and its consequences on UV impact. Int J Mol Sci 2018;19:2668.

Delevoye C, Marks MS, Raposo G. Lysosome-related organelles as functional adaptations of the endolysosomal system [published correction appears in Curr Opin Cell Biol 2019;61:141]. Curr Opin Cell Biol 2019;59:147−58.

Domingues L, Hurbain I, Gilles-Marsens F, Sirés-Campos J, André N, Dewulf M, et al. Coupling of melanocyte signaling and mechanics by caveolae is required for human skin pigmentation. Nat Commun 2020;11:2988.

Encarnação M, Espada L, Escrevente C, Mateus D, Ramalho J, Michelet X, et al. A Rab3a-dependent complex essential for lysosome positioning and plasma membrane repair. J Cell Biol 2016;213:631−40.

Escrevente C, Bento-Lopes L, Ramalho JS, Barral DC. Rab11 is required for lysosome exocytosis through the interaction with Rab3a, Sec15 and GRAB. J Cell Sci 2021;134:jcs246694.

Fitzpatrick TB, Breathnach AS. [The epidermal melanin unit system]. Dermatol Wochenschr 1963;147:481−9.

Fukuda M. Membrane traffic in the secretory pathway. Cell Mol Life Sci 2008;65:2801−13.

Hearing VJ. Biogenesis of pigment granules: a sensitive way to regulate melanocyte function. J Dermatol Sci 2005;37:3–14.

Hirobe T. Keratinocytes regulate the function of melanocytes. Dermatol Sin 2014;32:200–4.

Hong W. SNAREs and traffic [published correction appears in Biochim Biophys Acta 2005;1744:465]. Biochim Biophys Acta 2005;1744:120–44.

Hume AN, Ushakov DS, Tarafder AK, Ferenczi MA, Seabra MC. Rab27a and MyoVa are the primary Mlph interactors regulating melanosome transport in melanocytes. J Cell Sci 2007;120:3111–22.

Joshi PG, Nair N, Begum G, Joshi NB, Sinkar VP, Vora S. Melanocyte-keratinocyte interaction induces calcium signalling and melanin transfer to keratinocytes. Pigment Cell Res 2007;20:380–4.

Lagache T, Sauvonnet N, Danglot L, Olivo-Marin JC. Statistical analysis of molecule colocalization in bioimaging. Cytometry A 2015;87:568–79.

Lo Cicero A, Delevoye C, Gilles-Marsens F, Loew D, Dingli F, Guéré C, et al. Exosomes released by keratinocytes modulate melanocyte pigmentation. Nat Commun 2015;6:7506.

Marks MS, Seabra MC. The melanosome: membrane dynamics in black and white. Nat Rev Mol Cell Biol 2001;2:738–48.

Moreiras H, Pereira FJC, Neto MV, Bento-Lopes L, Festas TC, Seabra MC, et al. The exocyst is required for melanin exocytosis from melanocytes and transfer to keratinocytes. Pigment Cell Res 2019;33:366–71.

Moreiras H, Seabra MC, Barral DC. Melanin transfer in the epidermis: the pursuit of skin pigmentation control mechanisms. Int J Mol Sci 2021;22:4466.

Moreiras H, Bento-Lopes L, Neto MV, Escrevente C, Cabaço LC, Hall MJ, et al. Melanocore uptake by keratinocytes occurs through phagocytosis and involves protease-activated receptor-2 internalization. Traffic 2022;23:331–45.

Mosca S, Cardinali G, Flori E, Briganti S, Bottillo I, Mileo AM, et al. The PI3K pathway induced by αMSH exerts a negative feed-back on melanogenesis and contributes to the release of pigment. Pigment Melanoma Cell Res 2020;34:72–88.

Narayanan DL, Saladi RN, Fox JL. Ultraviolet radiation and skin cancer. Int J Dermatol 2010;49:978–86.

Olivo-Marin JC. Extraction of spots in biological images using multiscale products. Pattern Recognition 2002;35:1989–96.

Park HY, Kosmadaki M, Yaar M, Gilchrest BA. Cellular mechanisms regulating human melanogenesis. Cell Mol Life Sci 2009;66:1493–506.

Quevedo MF, Bustos MA, Masone D, Roggero CM, Bustos DM, Tomes CN. Grab recruitment by Rab27A-Rabphilin3a triggers Rab3A activation in human sperm exocytosis. Biochim Biophys Acta Mol Cell Res 2019;1866:612–22.

Raposo G, Marks MS. The dark side of lysosome-related organelles: specialization of the endocytic pathway for melanosome biogenesis. Traffic 2002;3:237–48.

Raposo G, Marks MS, Cutler DF. Lysosome-related organelles: driving post-Golgi compartments into specialisation. Curr Opin Cell Biol 2007;19:394–401.

Schindelin J, Arganda-Carreras I, Frise E, Kaynig V, Longair M, Pietzsch T, et al. Fiji: an open-source platform for biological-image analysis. Nat Methods 2012;9:676–82.

Scott G. Photo protection begins at the cellular level: microparasols on the job. J Invest Dermatol 2003;121:viii.

Scott G, Zhao Q. Rab3a and SNARE proteins: potential regulators of melanosome movement. J Invest Dermatol 2001;116:296–304.

Skoniecka A, Cichorek M, Tyminska A, Pelikant-Malecka I, Dziewiatkowski J. Melanization as unfavorable factor in amelanotic melanoma cell biology. Protoplasma 2021;258:935–48.

Taisuke K, Hearing JV. Update on the regulation of mammalian melanocyte function and skin pigmention. Exp Dermatol 2011;6:97–108.

Tarafder AK, Bolasco G, Correia MS, Pereira FJC, Iannone L, Hume AN, et al. Rab11b mediates melanin transfer between donor melanocytes and acceptor keratinocytes via coupled Exo/endocytosis [published correction appears in J Invest Dermatol 2020;140:1670] J Invest Dermatol 2014;134:1056–66.

Wäster P, Eriksson I, Vainikka L, Rosdahl I, Öllinger K. Extracellular vesicles are transferred from melanocytes to keratinocytes after UVA irradiation. Sci Rep 2016;6:27890.

Wu XS, Masedunskas A, Weigert R, Copeland NG, Jenkins NA, Hammer JA. Melanoregulin regulates a shedding mechanism that drives melanosome transfer from melanocytes to keratinocytes. Proc Natl Acad Sci USA 2012;109:E2101–9.

Yamaguchi Y, Hearing VJ. Physiological factors that regulate skin pigmentation. BioFactors 2009;35:193–9.

Zerial M, McBride H. Rab proteins as membrane organizers [published correction appears in Nat Rev Mol Cell Biol 2001;2:216] Nat Rev Mol Cell Biol 2001;2:107–17.

Zografou S, Basagiannis D, Papafotika A, Shirakawa R, Horiuchi H, Auerbach D, et al. A complete Rab screening reveals novel insights in Weibel–Palade body exocytosis. J Cell Sci 2012;125:4780–90.